Journal of the Serbian Society for Computational Mechanics / Vol. 2 / No. 1, 2008 / pp. 90-99

UDC: 519.642:532

On Accuracy of the Element-Free Galerkin (EFG) Method in Modeling Incompressible Fluid Flow

I. Vlastelica[1,2], V. Isailović[3], T. Djukić[4], N. Filipović[3,4], M. Kojić[*3,5,6]

[1] Technical High School, Čačak, Serbia
[2] Faculty of Information Technologies, Belgrade, Serbia
ivlastelica@sbb.co.yu
[3] Research and Development Center for Bioengineering 'BIOIRC', Kragujevac, Serbia
visailovic@kg.ac.yu; fica@kg.ac.yu
[4] Faculty of Mechanical Engineering, University of Kragujevac, Serbia
tijanakg@Eunet.yu
[5] Harvard School of Public Health, Boston, USA
[6] Department of Biomedical Engineering, University of Texas Medical Center at Houston, USA
mkojic@hsph.harvard.edu
**Corresponding author*

Abstract

Element-free Galerkin method (EFG) has been introduced in the nineties of last century (see e.g. Belytschko et al. 1994, 1996). It represents a mesh-free method, particularly suitable for problems where the FE method would need a remeshing procedure. The EFG has been mainly used in solid mechanics for problems involving change of the boundary, as in case of fracture propagation.

We have investigated applicability of the EFG in modeling incompressible fluid flow, especially the solution accuracy when various numbers of free points and integration schemes are employed. In this report we present our findings by analyzing solution of simple fluid flow examples: flow on a plate and flow in a cavity.

Keywords: Element-free Galerkin method, accuracy of fluid flow solutions, variation of number of free points, flow on a plate, flow in a cavity

1. Introduction

The finite element method (FE) is very well established and generally applicable. It has been developed and applied in almost all branches of science and technology. However, there are problems where the FE method shows some shortcomings. The main disadvantage and difficulty in application of the FE method are when a remeshing procedure is required during the solution process. Typical problems of this kind are when a fluid boundary significantly changes over time, as in case of moving solids through a fluid; or when boundaries change in the sold, as in case of fracture propagation.

The element free-Galerkin method (EFG) has been introduced to overcome the difficulties arising in the FE method applications (see e.g. Belytschko et al. 1994, 1996). The EFG idea consist basically in that a spatial field is interpolated over a certain points, called free-points, which do not belong to a mesh, as in the FE method. The interpolation relies on the vicinity criterion, i.e. a value of the interpolated quantity at a point within the modeling domain is affected by values at free points within a surrounding domain of a specified size. The key term in this interpolation is a weight function which decays with the distance, as graphically illustrated in Fig. 1.

The EFG is not totally mesh-free because a space mesh is required to perform integration over subdomains called EFG cells. The space integration is performed in a usual manner, as in the FE method, over integration points. A contribution to the governing matrices and vectors used to express balance laws, evaluated at an integration point, is added to the corresponding terms of the matrices and vectors of the discretized system of equations. During the solution procedure the number of free points belonging to an integration point might change, as well as the space cells, what offers a significant flexibility in modeling.

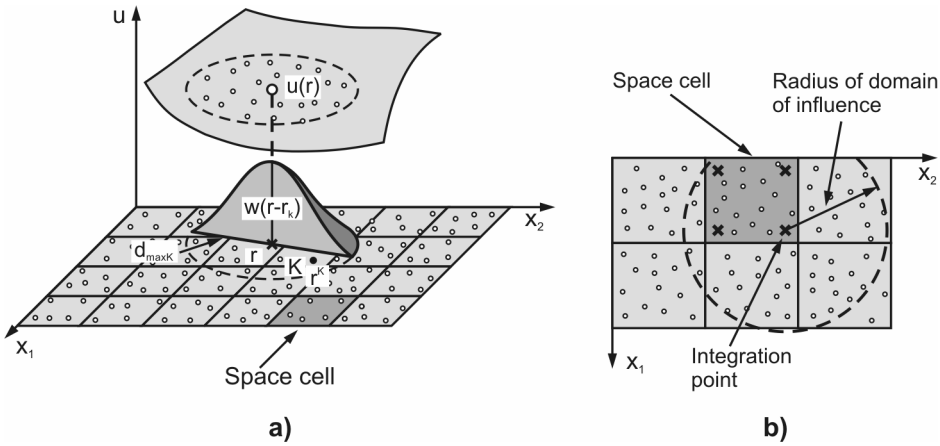

Fig. 1. Discretization of a function u (**r**) by the EFG method. (a) Schematic of discretization into space cells and use of free points ($w(\mathbf{r}-\mathbf{r}^K)$ is the weight function, K is a free point, $d_{\max K}$ defines the size of the domain of influence for the weight function $w\left(\mathbf{r}-\mathbf{r}^K\right)$); (b) Space cell used for integration and domain of influence around the integration point. According to Kojic et al. (2008a).

We summarize the basic equations of the EFG in the next section, followed by the incremental equations of balance for incompressible fluid; then we present accuracy analysis on two examples, and finally give concluding remarks at the paper.

2. Fundamental relations of the EFG

Consider a function $u(\mathbf{r})$ which represents a spatial field of a physical quantity. Here, $\mathbf{r}$ is a position vector of a point (which usually is a material point) with respect to a reference coordinate system. Then, the EFG approximation can be expressed as (Belytschko et al. 1994, 1996):

$$u(\mathbf{r}) = \sum_{j}^{m} p_j(\mathbf{r}) a_j(\mathbf{r}) \equiv \mathbf{p}^T(\mathbf{r}) \mathbf{a}(\mathbf{r}) \tag{1}$$

where $p_j(\mathbf{r})$ are the components of the base vector $\mathbf{p}(\mathbf{r})$, as monomials in the coordinates of $\mathbf{r}(x,y,z)$ so that the basis is complete; it is set that the component $p_1 = 1$; and m is the basis size. We need to determine the coefficients $a_j(\mathbf{r})$ and we proceed as shown further in the text. The linear and quadratic bases for one-dimensional space are

$$\mathbf{p}^T(\mathbf{r}) = [1, x], \text{ linear, } m = 2; \quad \mathbf{p}^T(\mathbf{r}) = [1, x, x^2], \text{ quadratic, } m = 3 \tag{2}$$

and for the 2D space we have

$$\begin{aligned} &\mathbf{p}^T(\mathbf{r}) = [1, x, y], && \text{linear} && m = 3 \\ &\mathbf{p}^T(\mathbf{r}) = [1, x, y, x^2, xy, y^2] && \text{quadratic} && m = 6 \end{aligned} \tag{3}$$

The coefficients $a_j(\mathbf{r})$ are determined by minimizing a weighted quadratic form

$$J = \sum_{K=1}^{n} w(\mathbf{r} - \mathbf{r}^K) \left[\mathbf{p}^T(\mathbf{r}^K) \mathbf{a}(\mathbf{r}) - U^K \right]^2 \tag{4}$$

where K denotes the free point number with the position vectors $\mathbf{r}^K$ and with the value of the function U^K; $w(\mathbf{r} - \mathbf{r}^K)$ is a weight function which decreases with the distance between a material point with position vector $\mathbf{r}$ and the free point K (see Fig.1); and n is the number of free points in the domain of influence around the material point. From the minimization of J with respect to the coefficients $a_j(\mathbf{r})$, we obtain the following system of equations:

$$\frac{\partial J}{\partial a_i} = 2 \sum_{K=1}^{n} w^K \left(p_j^K a_j - U^K \right) p_i^K = 0, \quad \text{sum on } j: j = 1, 2, ..., m \tag{5}$$

where $w^K \equiv w(\mathbf{r} - \mathbf{r}^K)$, $p_j^K \equiv p_j(\mathbf{r}^K)$. We further write this system of equations as

$$A_{ij} a_j - B_{iK} U^K = 0, \quad \text{sum on } K \text{ and } j: K = 1, 2, ..., n; j = 1, 2, ..., m \tag{6}$$

where the matrices **A** and **B** are:

$$A_{ij} = \sum_{J=1}^{n} w^J p_i^J p_j^J; \quad B_{iK} = p_i^K w^K, \quad \text{no sum on } K \tag{7}$$

The matrices **A** and **B** are of order $m \times m$ and $m \times n$, respectively. By solving the system (6) we obtain the coefficients $a_j(\mathbf{r})$:

$$\mathbf{a}(\mathbf{r}) = \mathbf{A}^{-1}\mathbf{B}\mathbf{U}; \quad \text{or} \quad a_j(\mathbf{r}) = \sum_{K=1}^{n} \left(\mathbf{A}^{-1}\mathbf{B} \right)_{jK} U^K \tag{8}$$

Substitution of $\mathbf{a}(\mathbf{r})$ from (8) into (1) gives the approximation for the function $u(\mathbf{r})$ as

$$u(\mathbf{r}) = \mathbf{p}^T \mathbf{A}^{-1} \mathbf{B} \mathbf{U} = \sum_{K=1}^{n} \Phi_K(\mathbf{r}) U^K \tag{9}$$

where the interpolation function $\Phi_K(\mathbf{r})$ corresponding to the free point *K*, is

$$\Phi_K(\mathbf{r}) = \sum_{j=1}^{m} \left(\mathbf{A}^{-1}\mathbf{B}\right)_{jK} p_j \tag{10}$$

The form (9) can further be used in all derivations of expressions needed in the governing equations, either for solid or fluid (see Section 3). Details how derivatives of the interpolation with respect to a Cartesian coordinates can be found elsewhere (e.g. Vlastelica 2003; Kojic et al. 2006, 2008a,b).

We further give two expressions for the weight functions: exponential and polynomial (Belytschko et al. 1994). The exponential form is

$$w^J\left(d_J^{2k}\right) = \begin{cases} \dfrac{\exp\left[-\left(d_J/c\right)^{2k}\right] - \exp\left[-\left(d_{\max J}/c\right)^{2k}\right]}{1-\exp\left[-\left(d_{\max J}/c\right)^{2k}\right]}, & d_J \le d_{\max J} \\ 0, & d_J \ge d_{\max J} \end{cases} \tag{11}$$

and the polynomial form is

$$w^J\left(d_J\right) = \begin{cases} 1-6\left(\dfrac{d_J}{d_{\max J}}\right)^2 + 8\left(\dfrac{d_J}{d_{\max J}}\right)^3 - 3\left(\dfrac{d_J}{d_{\max J}}\right)^4, & d_J \le d_{\max J} \\ 0 & d_J > d_{\max J} \end{cases} \tag{12}$$

where $d_J = \left\|\mathbf{r} - \mathbf{r}^J\right\|$ is the distance between the material point and the free point *J*; $d_{\max J}$ is the domain of influence for the weight function w^J; *k* is the parameter (in the examples here we use $k = 1$); and

$$c = \alpha \max\left\|\mathbf{r}_K - \mathbf{r}_J\right\| \qquad \text{for all free points} \tag{13}$$

where $1 \le \alpha \le 2$ is recommended.

3. Incremental-iterative EFG equations of balance for incompressible fluid

Here, we summarize a derivation of EFG equations of balance used in an incremental-iterative solution procedure. The steps in this derivation are analogous to those in the FE method (Kojic et al. 2008a).

The fundamental equation of balance of linear momentum is given as

$$\rho\left(\frac{\partial v_i}{\partial t} + v_{i.k}v_k\right) + \frac{\partial p}{\partial x_i} - \frac{\partial \tau_{ik}}{\partial x_k} - f_i^V = 0 \qquad i = 1,2,3;\ \text{sum on } k:\ k = 1,2,3 \tag{14}$$

where ρ is fluid density, v_i are velocity components, *p* is pressure, τ_{ik} are viscous stresses, and f_i^V are components of a body force (per unit volume). Now, we adopt interpolation for velocity and pressure as

$$\mathbf{v} = \mathbf{\Phi V}, \quad \text{or} \quad v_i = \Phi_K V_i^K; \quad \text{sum on } K,\ K = 1,2,....,n;\ \ i = 1,2,3 \tag{15}$$

and

$$p = \hat{\mathbf{\Phi}}\mathbf{P}, \quad \text{or} \quad p = \Phi_K P^K, \quad \text{sum on } K,\ K = 1,2,....,n \tag{16}$$

where $\mathbf{V}$ is the vector of velocities at free points in the domain of influence – its transpose is $\mathbf{V}^T \left[V_1^1 V_1^2 ... V_1^n ; V_2^1 V_2^2 ... V_2^n ; V_3^1 V_3^2 ... V_3^n \right]$; and $\mathbf{P}$ the vector of pressures at free points.

We next apply the Galerkin method according to which we multiply (14) by the interpolation functions $\Phi_K \left(\mathbf{r}, \mathbf{r}^K \right)$ (and use the Gauss theorem) to obtain the following balance equation in a matrix form

$$\mathbf{M}\dot{\mathbf{V}} + \hat{\mathbf{K}}_{vv}\mathbf{V} + \mathbf{K}_{vp}\mathbf{P} = \mathbf{F}_v - \mathbf{F}_\tau \tag{17}$$

where the matrices can be written in component form as

$$\left[M_{KJ} \right]_{ii} = \int_V \rho \Phi_K \Phi_J dV \tag{18}$$

$$\left[\left(\hat{\mathbf{K}}_{vv} \right)_{KJ} \right]_{ii} = \left[\rho \int_V \Phi_K \Phi_{J,j}\, v_j dV \right]_{ii} \tag{19}$$

$$\left[\left(\mathbf{K}_{vp} \right)_{KJ} \right]_{ii} = -\int_V \Phi_{K,i} \hat{\Phi}_J dV \tag{20}$$

The capital indices represent the free point numbers, while the indices *i* and *j* denote the coordinate numbers (=1,2,3). The terms of the nodal force vectors are:

$$\left(\mathbf{F}_v \right)_{Ki} = \int_V \Phi_K f_i^V dV + \int_S \Phi_K \left(-p\delta_{ij} + \tau_{ij} \right) n_j dS, \qquad \left(\mathbf{F}_\tau \right)_{Ki} = \int_V \Phi_{K,j} \tau_{ij} dV \tag{21}$$

where *V* is the volume the considered domain, and *S* is the surface bounding this domain. Note that the integral over the domain surface results in the force vector $\mathbf{F}_{vi}$; and summation of these vectors during the assemblage procedure leads to the cancellation, so that only the surface forces at the external boundaries remain.

A more common form of equation (17) is obtained with substituting the constitutive law for the viscous stress:

$$\tau_{ij} = 2\mu \dot{e}_{ij} = \mu \left(v_{i,j} + v_{j,i} \right) \tag{22}$$

where μ is the viscosity coefficient. Then equation (17) becomes

$$\mathbf{M}\dot{\mathbf{V}} + \mathbf{K}_{vv}\mathbf{V} + \mathbf{K}_{vp}\mathbf{P} = \mathbf{F}_v \tag{23}$$

where now the matrix $\mathbf{K}_{vv}$ is

$$\left[\left(\mathbf{K}_{vv} \right)_{KJ} \right]_{ii} = \left[\hat{K}_{KJ} \right]_{ii} + \left[K_{\mu KJ} \right]_{ii} \tag{24}$$

width

$$\left[K_{\mu KJ} \right]_{ii} = \int_V \mu \Phi_{K,j} \Phi_{J,j} dV \tag{25}$$

Also, this force vector can be expressed in terms of pressure and velocity on the boundary surface,

$$\left(\mathbf{F}_v\right)_{Ki} = \int_V N_K f_i^V dV + \int_S N_K \left(-p\delta_{ij} + \mu v_{i,j}\right) n_j dS \tag{26}$$

Equation (23) represents the Navier-Stokes equation in the EFG formulation.

To make the system of balance equations complete, we need to employ the continuity equation, now the continuity equation which for incompressible fluid is:

$$v_{i,i} = 0\,, \quad \text{or} \quad \frac{\partial v_1}{\partial x_1} + \frac{\partial v_2}{\partial x_2} + \frac{\partial v_3}{\partial x_3} = 0 \tag{27}$$

Multiplying this equation by the interpolation functions $\hat{\Phi}_K$, a weak form of the continuity equation is obtained as

$$\left(\int_V \hat{\Phi}_K \Phi_{J,J} dV\right) V_j^J = 0, \qquad \text{or} \qquad \mathbf{K}_{vp}^T \mathbf{V} = 0 \tag{28}$$

where the matrix $\mathbf{K}_{vp}$ is given in (20).

The system of equations (23) (or (17)) and (28) represent the system of EFG equations which can be assembled in a usual manner. The system is nonlinear since the matrix $\mathbf{K}_{vv}$ is nonlinear: it contains the velocity as the coefficient in $\left[K_{KJ}\right]_{ii}$. Therefore, an iterative scheme (see e.g. Kojic et al. 2008a) must be employed. For a time step '*n*' we obtain the following iterative form

$$\begin{bmatrix} \frac{1}{\Delta t}\mathbf{M} + {}^{n+1}\tilde{\mathbf{K}}_{vv}{}^{(i-1)} & \mathbf{K}_{vp} \\ \mathbf{K}_{vp}^T & \mathbf{0} \end{bmatrix} \begin{Bmatrix} \Delta\mathbf{V}^{(i)} \\ \Delta\mathbf{P}^{(i)} \end{Bmatrix} =$$
$$\begin{Bmatrix} {}^{n+1}\mathbf{F}_{ext}^{(i-1)} \\ 0 \end{Bmatrix} - \begin{bmatrix} \frac{1}{\Delta t}\mathbf{M} + {}^{n+1}\mathbf{K}_{vv}{}^{(i-1)} & \mathbf{K}_{vp} \\ \mathbf{K}_{vp}^T & 0 \end{bmatrix} \begin{Bmatrix} {}^{n+1}\mathbf{V}^{(i-1)} \\ {}^{n+1}\mathbf{P}^{(i-1)} \end{Bmatrix} + \begin{Bmatrix} \frac{1}{\Delta t}\mathbf{M}\,{}^{n}\mathbf{V} \\ 0 \end{Bmatrix} \tag{29}$$

where

$$\left[{}^{n+1}\left(\tilde{\mathbf{K}}_{vv}^{(i-1)}\right)_{KJ}\right]_{ik} = \left[{}^{n+1}K_{KJ}^{(i-1)}\right]_{ii} + \left[{}^{n+1}J_{KJ}^{(i-1)}\right]_{ik} \tag{30}$$

and

$$\left[{}^{n+1}J_{KJ}^{(i-1)}\right]_{ik} = \rho \int_V \Phi_K \, {}^{n+1}v_{i,k}^{(i-1)} \Phi_J dV \tag{31}$$

The equilibrium iterations stop when the norm of the incremental vector of the left-hand side, or the norm of the right-hand side (the 'unbalanced force') is smaller than a selected error tolerance.

4. Examples

In this section we present two examples to demonstrate effects of number of free points within an EFG cell and number of integration points on solution accuracy.

4.1Example 1 - Unsteady flow on a plate

We consider a 2D flow of incompressible flow caused by motion of a plate (Fig.2a). The dimension orthogonal to the plate is large (in the analytical model it is taken as infinity). Motion starts from the rest and motion of the plate by constant velocity v_0 propagates into the fluid producing the ultimate uniform fluid velocity in the vicinity of the plate, see the velocity profile in Fig. 2e denoted as stationary state.

EFG model is shown in Fig. 2b. We used the EFG cells shown in the figure and changed number of free points within each cell. We also used various number of integration points. In all these analyses the domain of influence was taken to be domain of the EFG cell.

The results are shown in Figs. 2c,d,e. Figures 2c and 2d show velocity fields for time $30s$ for 9 free points in EFG cells and 6×6 Gauss integration, and 4 free points in EFG cells and 4×4 Gauss integration, respectively. The linear basis (see (13)) is used for the velocity field and the exponential function (11) with $d_{\max J} = 2c$. It can bee seen that the field with more free points and more integration points is uniform along the field, while in the other case we have a disturbed velocity field. The increase in accuracy when the number of free points and integration points is increased, can be seen in the velocity profiles shown in Fig. 2e.

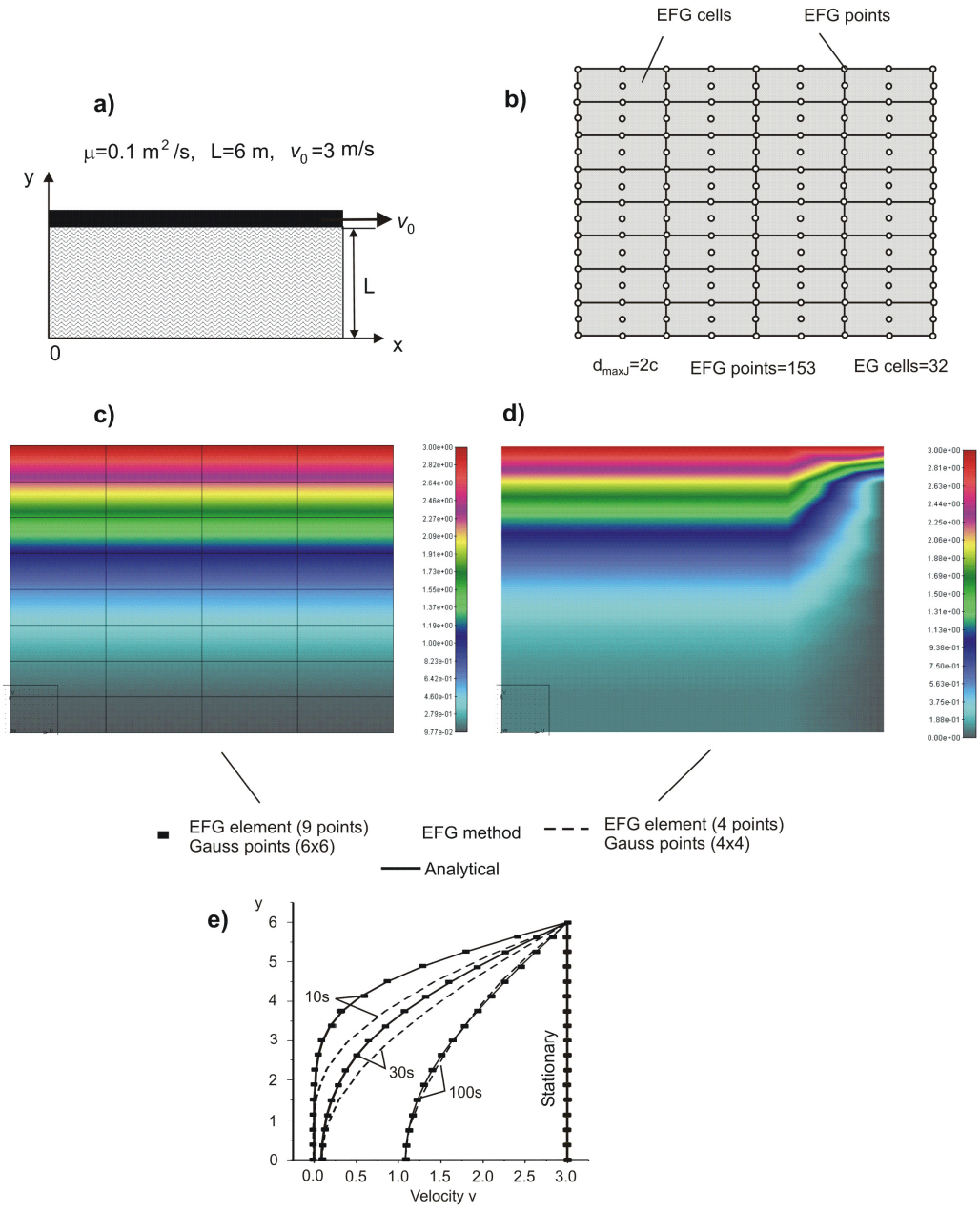

Fig. 2. Modeling of unsteady flow on a plate. (a) Geometry and material data; (b) EFG model; (c) and (d) Velocity field at time t=30s: (c) 9 free points in EFG cells and 6×6 Gauss integration, (d) 4 free points in EFG cells and 4×4 Gauss integration; (e) Velocity profiles during evolution of flow from the resting state to stationary conditions, EFG and analytical solutions.

4.2 Example 2 - Flow in a cavity

In this example we analyze fluid flow in a box (cavity). Motion of the fluid is caused by motion of the top boundary by constant velocity **v**, Fig. 3a. This example has been served as a benchmark example for testing solution methods of incompressible fluid flow, such as the finite element method (FE), dissipative particle dynamics (DPD), or multiscale procedure – coupling the DPD and FE methods (see, e.g. Kojic et. al. 2008a,b).

Here, we modeled this fluid flow by the EFG method. The mesh of the EFG cells and 8 free points belonging to a cell is shown in Fig. 3a. The linear basis (see (3)) is used for the velocity field and the exponential function (11) with $d_{\max,J} = 2c$. The fluid is initially at rest and the flow tends to ultimate stationary state.

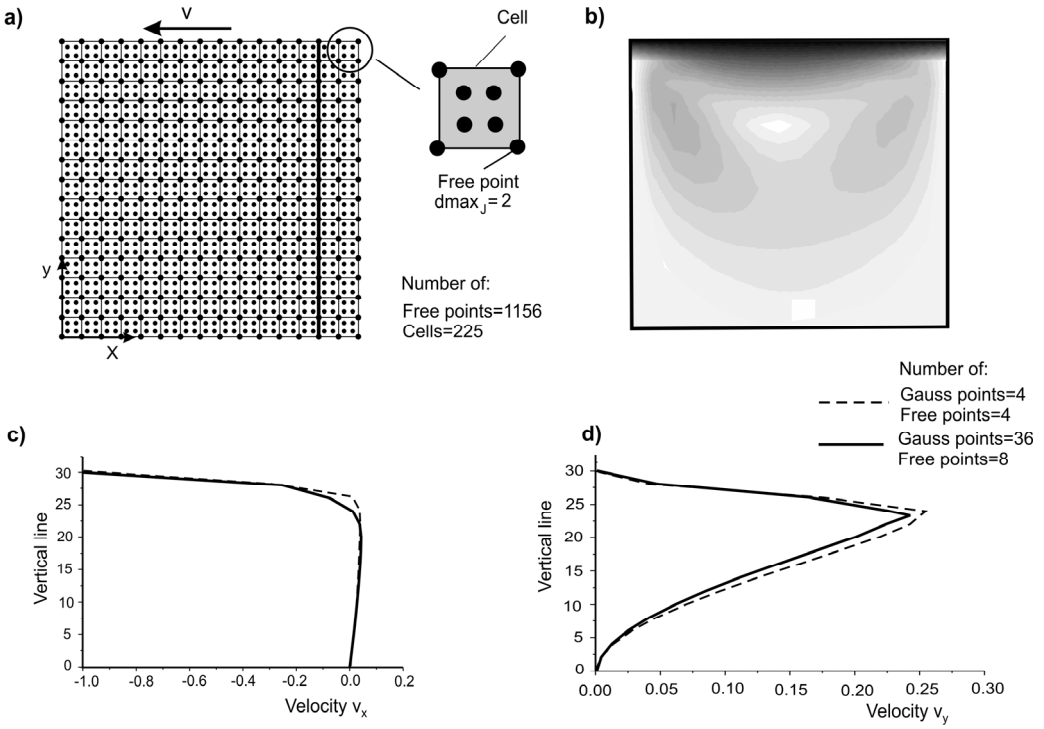

Fig. 3. EFG model of flow in a cavity. (a) Geometry, mesh of EFG cells and free points within a cell; (b) Field of velocity for time t=10 s.

We have explored solutions using various number of free points per cell and number of integration points. Solutions for the velocity distribution along a selected vertical line were compared for these variations of the model parameters. We have found that the solutions did not have significant variations and compare well with the FE solutions. Two of these solutions are shown in Fig. 3c,d, for time t=10 s. Velocity field for the same time t=10 s is shown in Fig. 3b. It can be seen that the velocity field has a well known vortex-type character.

5. Conclusions

We explored applicability of the EFG method to modeling incompressible fluid flow. The aim of this report also was to investigate solution accuracy when number of EFG free points changes within a cell. Also, solutions are compared when the number of integration points is changed. Our findings are illustrated on two examples.

It can be concluded that an increased number of free points per cell with increased number of integration points lead to more accurate results. From these EFG modeling features it follows that to improve solution accuracy, more computing efforts are required and therefore the method might be computationally inefficient. On the other hand, the EFG method have advantages in modeling problems where the FE method would need a remeshing.

Acknowledgements The authors acknowledge support of the Ministry of Science of Serbia, grant OI144-2/08; and City of Kragujevac, Contract 1224/08.

References

Belytschko T, Lu YY, Gu L (1994). Element-free Galerkin methods, *Int. J. Num. Meth. Engrg.*, 37, 229-256.

Belytschko T, Krongauz Y, Organ D, Fleming M, Krysl P (1996). Meshless Methods: An overview and recent developments, *Comp. Meth. Appl. Mech. Engrg.*, 139, 3-47.

Kojic M, Filipovic N, Tsuda A (2006). A multiscale method for bridging dissipative particle dynamics and Navier-Stokes finite element equations for incompressible fluid and its application in biomechanics. Proc. First South-East European Conference on Comp. Mechanics (Eds. M. Kojic and M. Papadrakakis), Kragujevac, Serbia.

Kojic M, Filipovic N, Stojanovic B, Kojic N (2008a). *Computer Modeling in Bioengineering* – Theory, Examples and Software, J. Wiley and Sons.

Kojic M, Filipovic N, Tsuda A (2008b). A mesoscopic bridging scale method for fluids andcoupling dissipative particle dynamics with continuum finite element method, *Comp. Meth Appl. Mech. Eng.*, 197, 821-833.

Vlastelica I. (2003). Methods of solving elastic-plastic deformation of nonporous and porous metal in fracture mechanics, Ph. Thesis (in Serbian), Faculty of Mechanical Engineering, University of Kragujevac.